

1 **A Mechanistic model to predict pressure drop and holdup pertinent to horizontal gas-**
 2 **liquid-liquid intermittent flow**

3 **P. Babakhani Dehkordi**

4 Politecnico di Milano, Department of Energy, via Lambruschini 4, 20156 Milan, Italy

5

6 **Nomenclature**

Symbols	Denotes	Unit
A	pipe cross-sectional area	m ²
A _f	area of film section occupied by liquid	m ²
A _g	area of film section occupied by gas	m ²
C	regression coefficient (eq. 31)	[-]
C _e	coefficient depending on pipe inclination (eq. 32)	[-]
D	pipe diameter	m
e _{ri}	average relative error	-
f _g , f _l , f _i	gas-wall, liquid-wall, and interfacial friction factors	-
f _{LM}	liquid mixture friction factor	-
f _s	mixture-wall friction factor	-
Fr	Froude number (eq. 30)	-
g	gravitational acceleration	m·s ⁻²
H _g	mean gas hold up	-
H _{lf} , H _{ls}	liquid holdup in film section and slug body	-
h _L	liquid height in film section	m
J _g , J _o , J _w	gas, oil, and water superficial velocity	m·s ⁻¹

J_L, J_t	total liquid and mixture superficial velocity	$m \cdot s^{-1}$
$J_{g,c}$	critical superficial velocity	$m \cdot s^{-1}$
J_{go}	superficial gas velocity corresponding to shortest slug length	$m \cdot s^{-1}$
L_b, L_s	bubble and slug body length	m
L_u	slug unit length	m
N_{Fr}	Froude number (eq. 21)	-
N_μ	Viscous number	-
Re_g, Re_l	gas and liquid Reynolds number in film section	-
Re_s	mixture Reynolds number in slug body	-
Re_{sl}	superficial liquid Reynolds number	-
S_f, S_g, S_i	liquid, gas, and interface perimeters	m
U_b	velocity of dispersed bubble in slug body	$m \cdot s^{-1}$
U_d	drift velocity	$m \cdot s^{-1}$
U_f	liquid velocity in film section	$m \cdot s^{-1}$
U_g	gas velocity in film section	$m \cdot s^{-1}$
U_l	liquid velocity in slug body	$m \cdot s^{-1}$
U_t	translational bubble velocity	$m \cdot s^{-1}$
$\Delta P/L$	three-phase pressure drop	Pa/m
α	coefficient depending on liquid height	-
ε	standard deviation of the relative errors	-
ε_{Lg}	ratio between gas to liquid superficial velocity	-
ε_{Lo}	ratio between oil to liquid superficial velocity	-
ε_{Lw}	ratio between water to liquid superficial velocity	-

ζ	distribution parameter	-
Θ	inclination angle	°
μ_{cont}	viscosity of continuous phase	Pa·s
μ_{g}	gas viscosity	Pa·s
μ_{L}	liquid viscosity	Pa·s
μ_{o}	oil viscosity	Pa·s
μ_{w}	water viscosity	Pa·s
μ_{s}	average mixture viscosity in slug body	Pa·s
ρ_{g}	gas density	kg·m ⁻³
ρ_{l}	liquid density	kg·m ⁻³
ρ_{o}	oil density	kg·m ⁻³
ρ_{s}	average mixture density in slug body	kg·m ⁻³
ρ_{w}	water density	kg·m ⁻³
σ_{ow}	interfacial tension between oil and water	N·m ⁻¹
$\tau_{\text{l}}, \tau_{\text{g}}, \tau_{\text{i}}$	liquid-wall, gas-wall, interface shear stresses	Pa
τ_{s}	mixture-wall shear stress in slug body	Pa
Φ	independent parameter	-
χ	Lockhart-Martinelli parameter	-

7

8

9

10

11

12

13 **1. Introduction**

14 Multiphase flow of high viscous oil-water and oil-water-gas within pipelines are a matter of high
15 importance for petroleum industry. In the last decades, there have been a large number of
16 research studies on oil-water flows in horizontal ducts, see for instance, Charles et al. (1961),
17 Arney et al. (1993), Grassi et al. (2008), Sotgia et al. (2008), Colombo et al. (2015, 2017), Loh
18 and Premanadham (2016), Shi et al. (2017), Babakhani (2017), and Babakhani et al. (2017a,
19 2017b, 2018). In many practical application though, the presence of gas together with oil and
20 water is unavoidable, it would be necessary to investigate and predict the pressure drop and
21 phase holdup during multiphase production at different flow conditions.

22 There are several experimental investigations on characterization of liquid-liquid-gas flows,
23 considering much lower oil viscosity. A large part of these studies were conducted on a large-
24 scale test facility (WASP) at Imperial College, London. Among them, studies by Acikgoz et al.
25 (1992), Hall (1992), Pan (1996), Odozi (2000), and Hewitt (2005) can be mentioned. In most of
26 these researches, oil viscosity varied from 4 mPa·s to 153 mPa·s in horizontal tubes ranging from
27 19 mm to 78 mm. The focus of their studies has been on flow pattern observation, considering
28 interaction between gas and oil/water mixture.

29 Low viscous oil-water-gas flow may differ from those of high viscous oil-water-gas flow due to
30 the fact that viscous forces might play an important role in the latter case. To the best of author'
31 knowledge, information mostly concerning to pressure drop, liquid holdup and flow pattern for
32 high viscous oil-water-gas is still lacking in the open literature: the author was able to find only
33 six contributions, which summarily described in the following.

34 Bannwart et al. (2004) used oil, water, air with volumetric fluxes (superficial
35 velocities) varying in the intervals of $J_o=0.01-2.5$ m/s, $J_w=0.04-0.5$ m/s, and $J_g=0.03-10$
36 m/s, respectively. Experimental tests were conducted with two different oil viscosities
37 in two facilities with horizontal and vertical pipe orientation: heavy crude oil ($\mu_o=3.4$
38 Pa·s, $\rho_o=970$ kg.m⁻³ at 20 °C) within 28.4 mm (Laboratory scale) i.d. pipe and very
39 heavy crude oil ($\mu_o=36.95$ Pa·s, $\rho_o=972.1$ kg.m⁻³ at 20 °C) within 77 mm (Field scale)
40 i.d. pipe. To evaluate the effect of gas phase, the results of pressure drop were
41 presented based on a parameter defined as the ratio between three-phase pressure drop
42 to oil-water pressure drop at the same oil and water volumetric fluxes.

43 The work by Bannwart et al. (2009) can also be cited, used similar pipe configurations
44 and test fluids as operated by Bannwart et al. (2004). They measured pressure drop and
45 observed flow patterns, leading to identification of Nine flow patterns in horizontal
46 pipe: Bubble gas-Bubble oil (B_g, B_o), Bubble gas-Annular oil (B_g, A_o), Bubble gas-
47 Intermittent oil (B_g, I_o), Bubble gas-Stratified oil (B_g, S_o), Intermittent gas-Bubble oil
48 (I_g, B_o), Intermittent gas-Annular oil (I_g, A_o), Intermittent gas-Intermittent oil (I_g, I_o),
49 Stratified gas-Bubble oil (S_g, B_o), Stratified gas-Stratified oil (S_g, S_o). In the whole
50 ranges of experimental conditions, water always were in the contact with pipe wall,
51 preventing oil from sticking to the pipe and promoting the occurrence of core-annular
52 flow. Furthermore, concerning pressure drop, they concluded that gas superficial
53 velocity has a significant influence on frictional pressure loss.

54 Poesio et al. (2009) studied the flow of gas, water, and oil with two viscosities of 0.9 and 1.2 Pa·s
55 at room temperature. Different pipe diameters were tested, including 21 mm, 28 mm and 40 mm

56 i.d. Flow pattern under investigation was slug flow. Oil, water and air superficial velocities are in
57 the ranges of $J_o=0.46-1.08 \text{ m}\cdot\text{s}^{-1}$, $J_w=0.04-0.67 \text{ m}\cdot\text{s}^{-1}$, and $J_g=0.06-4 \text{ m}\cdot\text{s}^{-1}$. The main measurement
58 included pressure drop detected 6 m downstream of injector. They developed a hybrid model
59 which computes overall pressure drop based on Lockhart-Martinelli model and the results of
60 comparison between pressure drop predictions and measurements showed a fairly good
61 agreement.

62 The work by Wang et al. (2013) deals with oil-water-gas flowing in a horizontal pipe
63 with 52.5 mm i.d. pipe. Oil viscosity varied from 0.15 Pa.s to 0.57 Pa.s at temperatures
64 ranging from 37.8 to 15.6 °C, respectively. Oil, water, superficial velocities were
65 experimented up to 1 $\text{m}\cdot\text{s}^{-1}$, respectively, while gas superficial velocity was in the range
66 of 1 to 5 $\text{m}\cdot\text{s}^{-1}$. The flow patterns were observed and images recorded using high speed
67 video camera. They classified three-phase flow according to the interactions between
68 gas and liquid, and oil-water mixture within slug body and film regions, leading to four
69 different flow patterns: INT (O/W-S&SOW-F): gas and liquid are in slug flow (Oil is
70 dispersed in water within slug body and both are stratified in the film region); INT
71 (O/W-S & O/W-F): gas and liquid are in slug flow (Oil is dispersed in water in slug
72 body and film regions); INT (W/O-S & W/O-F): gas and liquid flow regime is slug
73 (Water is dispersed in oil in both slug body and film regions); STR (O/W-F): gas and
74 liquid flow regime is stratified (Oil and gas are entrained and dispersed in water, a thin
75 layer of oil is also present at the pipe wall). Moreover, pressure drop measurements
76 were performed and reported as a function of the water cut (defined as the ratio
77 between superficial water velocity to superficial liquid velocity), showing increased
78 trend of frictional pressure loss as gas velocity is increased.

79 Shmueli et al. (2015) investigated viscous oil-water-gas ($\mu_o=0.102$ Pa.s at 20 °C;
80 $\rho_o=847.9$ kg.m⁻³) flow within a horizontal pipe with 69 mm i.d. pipe and 50 m long.
81 Flow patterns were detected to be stratified-annular flow over the tested operating
82 conditions. Liquid height, phase hold up and pressure gradients were measured by
83 means of a traversing two-energy gamma densitometer. They concluded that there is a
84 curvy interface between gas and liquid, which is contrary to the visual observations.

85 Babakhani (2017) measured experimental pressure drop for three-phase flow within horizontal
86 40 mm i.d. pipe, considering $\mu_o=0.838$ Pa.s. In addition, Translational bubble velocity and
87 geometrical characteristics of slug units were determined by means cross-correlation of the
88 signal from two optical probes and video analysis. Based on experimental data, a new correlation
89 to compute the slug unit length as a function gas and liquid superficial velocity as well as pipe
90 diameter was suggested. Acceptable agreement between predicted slug unit length and
91 measurements was observed. A summary of experimental studies on viscous oil-water-gas flows
92 is listed in Table 1.

93 The most common flow pattern for oil-water-gas flows is slug flow, where a series of liquid
94 slugs is separated by relatively large gas pockets. Up to our knowledge, there are few theoretical
95 studies to characterize flow behavior of oil-water-gas flows, which is mostly related to stratified
96 flow regime (see Taitel et al., 1995, Khor et al., 1997, Hanich and Thompson, 2001). Taitel et al.
97 (1995) presented a theoretical approach for three layer stratified flow of liquid-liquid-gas to
98 compute liquid and gas holdup. Steady state momentum equations for each phase were written
99 and solution iteratively obtained by assuming a guess value for liquid height, that is, $h_L=h_w+h_o$.
100 Once solution for liquid height was obtained, other important physical parameters of flow such
101 as pressure drop and phase velocity can be calculated. The weakness of model is that is only

102 applicable to stratified three phase flow. Later, Khor et al. (1997) compared stratified
103 experimental data of liquid hold up with above model, considering different correlations for gas-
104 wall shear stress, oil-water and water-wall shear stresses. They found satisfactory agreement
105 between measured liquid holdup and prediction by the model.

106 Perhaps, the most complete work presented so far corresponding to Intermittent flow of
107 three phases is the unified model developed by Zhang and Sarica (2006), which was
108 presented after their proposed model for two-phase flow (see Zhang et al., 2003a).
109 They divided slug unit into two sections, including slug body and gas pocket regions,
110 assuming that oil and water are stratified in the gas pocket section. The model was
111 tested against experimental pressure drop data of Hall (1992), Laflin and Oglesby
112 (1976) where low oil viscosities were used ($\mu_o=0.005-0.083$ Pa·s). Preliminary
113 validations have been obtained between pressure drop prediction and measurements.
114 Performance of the mechanics model is also compared against experimental data of
115 Wang et al. (2013). However, the model was not able to predict high viscous oil-water-
116 gas flows, probably due to the fact that oil and water is considered to be stratified flow
117 regime in gas pocket region, which is not the case in the whole range of experimental
118 data.

119 In the original Unified model proposed by Zhang et al (2003a), the length of liquid in film
120 section (L_b) was either obtained based on trial and error procedure or from experimental data.
121 Furthermore, the value of liquid holdup in slug body region (H_{ls}) was calculated in an iterative
122 process. Hence, two numerical procedures are needed to compute L_b and H_{ls} . In the current work,
123 by knowing that $L_b=L_u-L_s$, modifications are suggested to the Unified model so that L_b can be
124 calculated, taking into account a correlation to compute total slug unit length (L_u) developed by

125 Babakhani (2017) for viscous oil-water-gas flow. By doing so, the complexity level of original
 126 Unified model is reduced. Another initiative of this study is that oil and water are summed to
 127 behave homogeneously, concerning flow regime under investigation (Slug flow with fully mixed
 128 oil/water and Slug flow with oil core/annular water). Hence, oil-water-gas three phase flow can
 129 be simplified into gas-liquid flow. In the following, a detailed description of the proposed
 130 mechanistic model for slug flow with different oil/water interactions is reported in section 2. The
 131 results of pressure drop prediction from mechanistic model are compared with experimental data
 132 banks of Poesio et al. (2009) and Babakhani (2017), as shown in section 4. It has to be remarked
 133 that all the available data were taken in plants with a “smooth” introduction of the phases and the
 134 measurements reported averages of the major quantities (phase holdup and pressure drop), which
 135 are independent of time, i.e. in quasi-steady state conditions.

136 **Table 1.** Summary of previous studies on viscous oil-water-gas flow in horizontal pipe

Author	Pipe I.D. (mm)	Pipe length (m)	μ_o (mPa·s)	ρ_o (kg·m ⁻³)	Velocity range (m·s ⁻¹)
Bannwart et al. (2004)	28.4;77	5.40 274	3400; 36950	970	J_o : 0.01-2.5 J_w : 0.04-0.5 J_g =0.03-10
Bannwart (2009)	28.4; 77	5.40 274	3400; 36950	970	J_o : 0.01-2.5 J_w : 0.04-0.5 J_g =0.03-10
Poesio et al. (2009)	21;28;40	9	900;1200	886	J_o : 0.46-1.08 J_w :0.04-0.67 J_g =0.06-4.0
Wang et al. (2013)	52.5	24	150-570	884.4	J_o :0.1-1 J_w :0.1-1 J_g =1-5
Shmueli et al. (2015)	69	50	102	847.9	J_o :0.05-0.8

					$J_w:0.05-0.8$
					$J_g=1.3-10.7$
Babakhani (2017)	40	12	838	890	$J_o:0.36-0.71$
					$J_w:0.44-1.32$
					$J_g=0.22-2.10$

137

138 **2. Mechanistic model**

139 The idea of considering oil and water mixture as a homogeneous flow for dispersed
140 flow regime was presented by Picchi et al. (2015) for oil-water flows, where a steady
141 two-fluid model is used to predict pressure gradient and phase holdup. This concept is
142 extended for three-phase slug flow, making use of Zhang et al. (2003a) mechanistic
143 model. Essentially, prediction by mechanistic models is more accurate than general
144 correlations regardless of the number of phases within pipeline because most important
145 hydrodynamic parameters are considered.

146 **2.1 Mass conservation equations**

147 The mathematical model presented here is based on the slug unit cell propagating with
148 the translational velocity (U_T) in horizontal pipe proposed by Zhang et al. (2003a). The
149 schematic geometry of slug is depicted in Fig. 1. The slug unit cell is divided into two
150 sections: a liquid slug body with a length of L_s and a film section with elongated
151 bubble length of L_b where gas and liquid are stratified. The slug body contains gas
152 entrainment in the form of dispersed bubbles, on the other hand, no liquid is entrained
153 and dispersed into the gas pocket. Thus, the current hybrid model is a combination of a
154 two-fluid model for the segregated flow part and a drift-flux model for the dispersed
155 component. The model is a steady state model in which liquid and gas are treated as

156 incompressible flows. This assumption is still valid even for long pipelines where the
 157 density is not constant, see Taitel and Barnea (1990). In order to make use of two-fluid
 158 model in the film section with characteristic length of L_b , a homogeneous distribution
 159 of liquid phases is assumed and the effective viscosity of liquid is calculated according
 160 the Einstein's equation (1906):

$$161 \quad \mu_L = \mu_{\text{cont}}(1 + 2.5 \varepsilon_{Lo}) \quad (1)$$

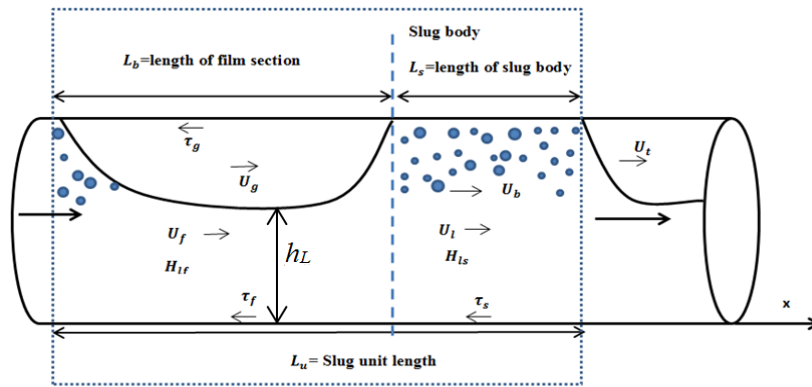
162 Where μ_{cont} and ε_o are viscosity of continuous phase (water) and input volume oil
 163 fraction ($\varepsilon_{Lo} = \frac{J_o}{J_L} = 1 - \varepsilon_{LW}$), respectively. The application of eq. 1 requires that
 164 spherically dispersed bubbles are distributed evenly in a radial direction. In the present
 165 study, the combined continuity and momentum equations for gas/two phase liquid is
 166 adopted. If a reference frame with the same velocity as U_t is considered, the mass
 167 balance for both liquid and gas phases can be written by considering the liquid and gas
 168 mass flow rates entering and exiting control volume:

$$169 \quad H_{ls}(U_t - U_l) = H_{lf}(U_t - U_f) \quad (2.a)$$

$$170 \quad (1 - H_{ls})(U_t - U_b) = (1 - H_{lf})(U_t - U_g) \quad (2.b)$$

171 Where U_l , U_b are liquid and bubble velocities in slug body and U_f , U_g are velocities of
 172 liquid and gas in gas pocket (film section). The dispersed bubble velocity in slug body
 173 can be estimated by model of Wallis (1969) which is a drift-flux based approximation
 174 as $U_b = 1.2 \cdot J_t$.

175



176

177

Fig 1. Schematic of slug flow structure

178 When a slug unit cell passes, the following equations can be written for gas and liquid:

179
$$L_u J_l = L_s H_{ls} J_t + L_b H_{lf} U_f \quad (3)$$

180
$$L_u J_g = L_s (1 - H_{ls}) J_t + L_b (1 - H_{lf}) U_g \quad (4)$$

181
$$L_u = L_s + L_b \quad (5)$$

182 The mean average gas holdup can be calculated based on following equation:

183
$$H_g = \frac{J_g}{U_g} \quad (6)$$

184 **2.2 Momentum equations**

185 For the sake of simplicity, the liquid height and its shape (h_L) along the liquid film is
 186 considered to be uniform. The shape of liquid film requires a special attention, because,
 187 at the bubble front the liquid holdup gradient differs from that at the bubble tail.

188 Referring to Fig. 1, momentum equations can be derived according to the analysis of
 189 forces exerted at the inlet and out of control volume containing important information
 190 such as pressure loss. The entire film section as control volume is considered and

191 momentum equations solved, see for instance, Zhang et al. (2003a). The momentum
 192 equation for liquid and gas pocket in horizontal pipe is given by:

$$193 \frac{\rho_l(U_t-U_f)(U_t-U_f)}{L_b} = \frac{\Delta p}{L_b} + \frac{\tau_f S_f}{A_f} - \frac{\tau_i S_i}{A_f} - \rho_l g \cos \theta \frac{\partial h_L}{\partial x} \quad (7)$$

$$194 \frac{\rho_g(U_t-U_g)(U_b-U_g)}{L_b} = \frac{\Delta p}{L_b} + \frac{\tau_g S_g}{A_g} - \frac{\tau_i S_i}{A_g} - \rho_g g \cos \theta \frac{\partial h_L}{\partial x} \quad (8)$$

195 The pressure drop terms and the last term in RHS of eq. 7 and 8 are eliminated from
 196 above equations. Thus, the combined momentum equation may be given by:

$$197 \frac{\rho_l(U_t-U_f)(U_t-U_f) - \rho_g(U_t-U_g)(U_b-U_g)}{L_b} - \frac{\tau_f S_f}{A_f} + \frac{\tau_g S_g}{A_g} + \tau_i S_i \left(\frac{1}{A_f} + \frac{1}{A_g} \right) = 0 \quad (9)$$

198 The first term at LHS of equation (9) is the force due to momentum exchange between
 199 slug body and film section of unit. Zhao and Yeung (2015) reported that If there is low
 200 liquid film height (h_L in Fig 1), there is no considerable difference between gas pocket
 201 velocity (U_g) and liquid velocity in the film region (U_f) beneath it. Zhang and Sarica
 202 (2006) developed a unified model, taking into account the stratified gas-oil-water in
 203 both liquid slug body and film sections. They stated that L_b tends to be infinitely long
 204 in stratified flow of gas-oil-water. Thus, the momentum exchange term is neglected
 205 from equation (9), the original form of momentum equation, developed by Taitel and
 206 Barnea (1990) can be obtained. It is worth noting that liquid height calculated in this
 207 way is the one in its equilibrium level and can be iteratively computed according to
 208 equation 9.

209 Gas-wall (τ_g), liquid-wall (τ_f) and interfacial shear stresses between gas pocket and
 210 liquid in film region are defined as:

$$211 \quad \tau_f = f_l \frac{\rho_l U_f^2}{2} \quad (10)$$

$$212 \quad \tau_g = f_g \frac{\rho_g U_g^2}{2} \quad (11)$$

$$213 \quad \tau_i = f_i \frac{\rho_g (U_g - U_f) |U_g - U_f|}{2} \quad (12)$$

214 To calculate shear stresses in film region, some geometrical parameters are required which are
 215 given in Appendix A. The friction factors in equations 10-12 can be directly linked to the
 216 phase Reynolds number for liquid film and gas pocket:

$$217 \quad Re_l = \frac{4 A_f U_f \rho_L}{S_f \mu_L}, \quad Re_g = \frac{4 A_g U_g \rho_g}{(S_g + S_i) \mu_g} \quad (13)$$

218 In definition of gas Reynolds number, the cord length at the interface, S_i is used as
 219 suggested by Taitel and Dukler (1976).

220

221 **2.3 Pressure gradient prediction**

222 The total pressure drop for slug unit length can be computed using three contributions
 223 as frictional, gravitational and acceleration pressure gradients:

$$224 \quad -\frac{dP}{dx} = -\left(\frac{dP}{dx}\right)_F - \left(\frac{dP}{dx}\right)_G - \left(\frac{dP}{dx}\right)_A \quad (14)$$

225 We assumed that gas expansion would not occur from the entrance to downstream of
 226 pipeline (flow is incompressible) and acceleration contribution is negligible. Thus, the
 227 only contribution that remains is frictional term in horizontal pipe and computed as:

$$228 \quad -\left(\frac{dP}{dx}\right)_F = \frac{\tau_s \pi D}{A} \frac{L_s}{L_u} + \frac{\tau_f S_f + \tau_g S_g}{A} \frac{L_b}{L_u} \quad (15)$$

229 The first term in equation above corresponds to frictional pressure drop in slug body
230 and the second is frictional contribution to the pressure drop in the film zone.
231 Rheological properties of mixture in slug zone are calculated based on weighted
232 average of liquid and gas holdup, as proposed by Taitel and Barnea (1990) and Zhao
233 and Yeung (2015)

$$234 \quad \rho_s = H_{ls}\rho_l + (1 - H_{ls})\rho_g \quad (16)$$

$$235 \quad \mu_s = H_{ls}\mu_l + (1 - H_{ls})\mu_g$$

236 The shear stress in slug body caused by interaction between homogeneous mixture
237 (dispersed bubble entrained to slug body zone and liquid) and pipe wall in slug region,
238 τ_s , is calculated considering total mixture superficial velocity for Reynolds number:

$$239 \quad Re_s = \frac{\rho_s J_t D}{\mu_s} \quad (17)$$

$$240 \quad \tau_s = f_s \frac{\rho_s J_t^2}{2} \quad (18)$$

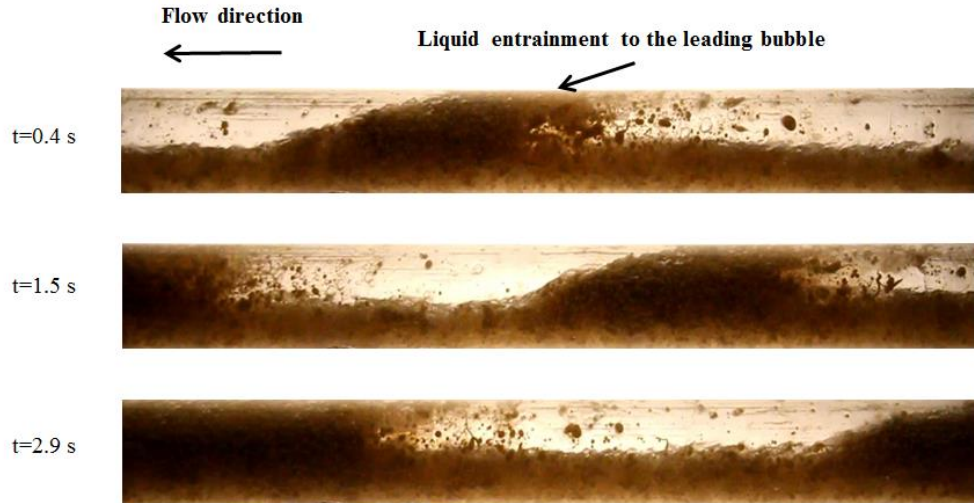
241 To compute pressure drop and phase holdup in high viscous oil-water-gas flow based
242 on mechanistic model presented in sections 2-1 to 2-3, some information are required,
243 including slug body holdup (H_{ls}) and length (L_s), and closure relation for two-phase
244 friction factor and translational velocity. All information is obtained from available
245 models in the literature for gas-liquid flow due to the lack of suitable models for three-
246 phase flow in horizontal pipes, discussed in sections 2.4 to 2.6. In addition to above
247 parameters, an appropriate model for slug unit length is necessary to calculate actual
248 velocity of phases and avoid iterative procedure in continuity equations. In the present

249 study, a new formulation for computing the total unit length as a function of pipe
250 diameter, and flow conditions are presented, explained in section 2.7.

251

252 **2.4 Slug body holdup**

253 The mechanistic model requires the information of slug body holdup. Some researchers
254 have studied liquid body holdup for gas-liquid flow in the case of low viscosity oil, see
255 for instance, Andreussi et al. (1993) and Nadler and Mewes (1995). The slug body
256 region can be divided into two sub-regions, namely, developed body region and
257 developing mixing region. When liquid moves from the layer beneath gas pocket to
258 slug region, a sudden expansion occurs which, in turn, helps to form a jet and create a
259 mixing region at the head of slug. As a result of mixing developing region and liquid
260 loss, the generated liquid re-circulate from slug body and move toward the leading
261 Taylor bubble tail. The rest of liquid is transported to the developed slug region (see
262 Fig. 2 taken from Babakhani, 2017). This phenomenon has significant effect on the
263 developing mixing length and its intensity as well as slug body liquid holdup.



264

265 **Fig 2.** Frames of subsequent images to show the liquid entrainment mechanism, image
 266 from Babakhani, 2017.

267 Al-Safran et al. (2015) experimentally examined the influence of high liquid viscosity
 268 on slug liquid holdup in horizontal pipe. They concluded that viscous and inertia forces
 269 are responsible for bubble loss, fragmentation (changing the size of larger bubbles to
 270 dispersed bubbles) in slug body. According to their work, increase in liquid viscosity
 271 would result in increasing slug body liquid holdup. A new formulation for slug body
 272 liquid holdup was presented as:

$$273 \quad H_{ls} = 0.85 - 0.075 \varphi + 0.057 \sqrt{\varphi^2 + 2.27} \quad (19)$$

$$274 \quad \varphi = N_{Fr} N_{\mu}^{0.2} - 0.89 \quad (20)$$

$$275 \quad N_{Fr} = \frac{J_t}{(gD)^{0.5}} \sqrt{\frac{\rho_L}{(\rho_L - \rho_g)}} \quad (21)$$

$$276 \quad N_{\mu} = \frac{J_t \mu_L}{g D^2 (\rho_L - \rho_g)} \quad (22)$$

277 2.5 Slug body length

278 In this section, comparisons have been made between experimental data of slug length
279 (measured by optical sensor) from Babakhani (2017) and empirical correlations
280 developed for viscous liquid-gas flow in the open literature, reported in Table 2. The
281 results of comparisons are depicted in Fig. 3 (a-b). Among the models presented in
282 Table 2, correlation by Barnea and Brauner (1985) has not been compared with
283 experimental data because it was developed for low viscous liquid-gas flows, its
284 application would lead to large overestimation of slug length. Furthermore, it is evident
285 from Fig. 3 (a-b) that model by Al-safran et al. (2011) is insensitive to superficial gas
286 velocity whilst slug length is immensely affected by gas velocity. It is worth remarking
287 that weighted averages are defined for liquid density and viscosity. They concluded
288 that average value of $L_s=10D$ is a reasonable approximation for viscous oil-gas
289 intermittent flow. In Fig. 3-b, an increase in slug length is observed at $J_g=0.95 \text{ m}\cdot\text{s}^{-1}$,
290 which is associated with increase in water cut (ϵ_{Lw}). When water (lower viscous phase)
291 is added, turbulent kinetic energy overcomes viscous forces and slug front becomes
292 more turbulent, more liquid is entrained into gas pocket from slug, which result in
293 stretching slug into longer slugs. This phenomenon is in agreement with the prescribed
294 behaviour in the works of Al-Safran et al. (2011) and Losi et al. (2016b). Losi et al.
295 (2016b) measured slug length for high viscous oil-air within a horizontal pipe. From
296 Fig. 3 (a-b), it can be seen that the approach by Losi et al. (2016b) is able to describe
297 the behavior of experimental data, particularly at low superficial gas velocity where
298 transition from slug to dispersed flow regime occurs. In the whole ranges of operating
299 conditions, average relative error between experimental data and model by Losi et al.

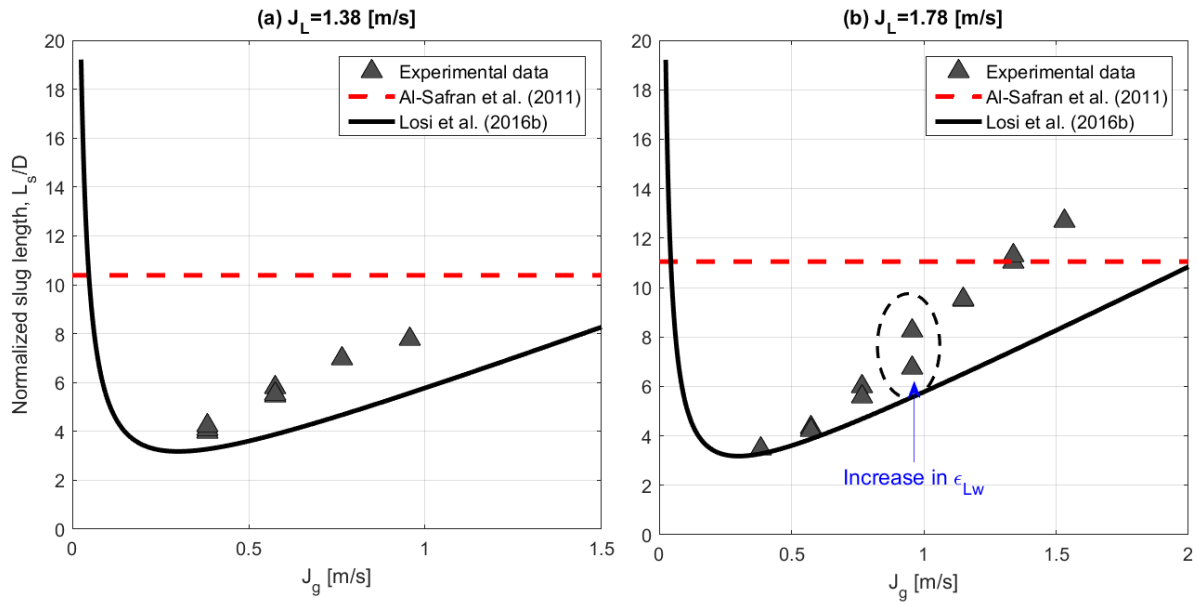
300 (2016b) is found to be 20.8%, with larger deviation at higher superficial gas velocity.
 301 The lower average relative error of Losi et al. (2016b) model might be related to
 302 considering both pipe diameter and superficial gas velocity as compared to other
 303 empirical correlations in the open literature. Hence, this model is used as an input in
 304 the mechanistic model for prediction of slug length.

305

306 **Table 2.** Slug length models for viscous liquid-gas flows from literature

Author	model	Additional information
Barnea and Brauner (1985)	$\frac{l_s}{D} = 32$	
Al-Safran et al. (2011)	$\frac{l_s}{D} = 2.63 \left(\frac{D^{3/2} \sqrt{\rho_l(\rho_l - \rho_g)g}}{\mu_l} \right)^{0.321}$	$\rho_l = \rho_w \varepsilon_{LW} + \rho_o \varepsilon_{Lo}$ $\mu_l = \mu_w \varepsilon_{LW} + \mu_o \varepsilon_{Lo}$
Losi et al. (2016b)	$\frac{l_s}{D} = K \left(J_g + \frac{J_{go}^2}{J_g} \right)$	$K = 5.3$ $J_{go} = 0.3$

307



308

309 **Fig. 3** Comparison between measured slug length (Babakhani, 2017) at (a) $J_L=1.38$
 310 m/s, (b) $J_L=1.78$ m/s and the predictions of Al-Safran et al. (2011) and Losi et al.
 311 (2016b)

312 2.6 Closure relation

313 2.6.1 Two phase friction factor

314 Some empirical correlations to express two phase friction factors as a function of phase
 315 Reynolds number is required. For gas-wall friction factor, Blasius formulation is often
 316 used as described by Taitel and Dukler (1976). The validity of gas-liquid friction
 317 factors estimated by Blasius is assessed by Khor et al. (1997) for three phase stratified
 318 flow. These are:

319 $f_g = \frac{16}{Re_g} \quad Re_g \leq 2100 \quad (23)$

320 $f_g = \frac{0.046}{Re_g^{0.2}} \quad Re_g > 2100 \quad (24)$

321 Zhao et al. (2013b) developed a new expression for liquid-wall friction factor in the
 322 case of laminar liquid for gas-liquid flow over the large range of liquid viscosity

323 $f_l = \frac{20.76}{Re_l} \quad \text{for} \quad Re_l \leq 2100 \quad (25)$

324 Kowalski (1987) measured wall-to-liquid shear stresses and proposed a new correlation
 325 for turbulent liquid-wall friction factor as a function of liquid superficial Reynolds
 326 number and local liquid holdup for the large range of phase superficial velocity.

327 $f_l = \frac{0.0262}{(H_{lf} Re_{sl})^{0.139}} \quad \text{for} \quad Re_l > 2100 \quad (26)$

328 Regarding interfacial friction factor, no dependence of gas-wall shear stresses on
 329 interfacial characteristic of gas-liquid in film region was observed, see for instance
 330 Taitel and Dukler, 1976 and Kowalski (1987).

331 Andritsos and Hanratty (1987) studied the effect of large-amplitude wave on interfacial
 332 conditions of gas-liquid flows and concluded that interfacial shear stresses increases as
 333 a result of higher large-amplitude wave. They defined a critical superficial velocity at
 334 which large amplitude wave appears and proposed a new correlation as a function of
 335 non-dimensional liquid height and superficial gas velocity.

336 $\frac{f_i}{f_g} = 1 \quad \text{for} \quad J_g \leq J_{g,c} \quad (27)$

337 $\frac{f_i}{f_g} = 1 + 15 \left(\frac{h_L}{D}\right)^{0.5} \left(\frac{J_g}{J_{g,c}} - 1\right) \quad \text{for} \quad J_g > J_{g,c}$

338 $J_{g,c} = 5 \left(\frac{\rho_{g0}}{\rho_g} \right)^{0.5}$ (28)

339 Where ρ_{g0} is the gas density at atmospheric pressure.

340

341 **2.6.2 Translational velocity of elongated bubble**

342 Translational bubble velocity was first presented by Nicklin (1962) as a function of
343 superficial mixture velocity (J) and drift velocity (U_d), based on drift-flux approach:

344 $U_t = \zeta \cdot J + U_d$ (29)

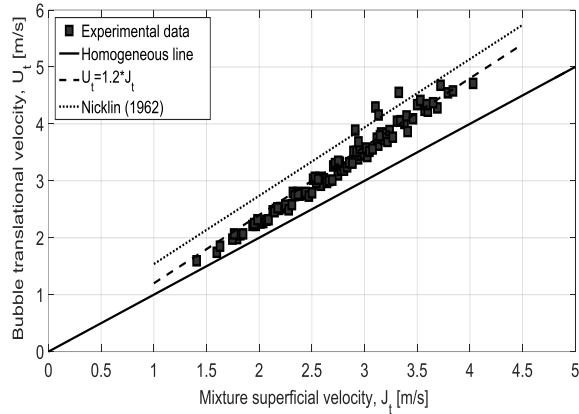
345 The other empirical correlations in the previous studies to calculate translational bubble
346 velocity are the modification of Nicklin (1962) model. The distribution parameter, ζ
347 was found to be 1.2 when flow is turbulent and 2 in the case of laminar flow. Benjamin
348 (1968) suggested that drift velocity can be correlated to Froude number, diameter and
349 gravitational acceleration in horizontal pipe.

350 $Fr = \frac{U_d}{\sqrt{gD}} = 0.54$ (30)

351 However, this correlation does not take into account viscous effect. Losi and Poesio
352 (2016) evaluated the influence of oil viscosity on drift velocity of a gas bubble in
353 liquids for different axial positions in both horizontal and inclined pipes. They
354 concluded that drift velocity for very viscous oil-gas flow ($\mu_o=0.804$ Pa·s) is ranged
355 between 0.0025-0.0065 m·s⁻¹ for different axial positions in a horizontal pipe, which
356 can be approximated equal to zero. Fig. 4 shows translational bubble velocity data from
357 Babakhani (2017), measured by optical sensor, as a function of mixture superficial

358 velocity. The square symbols denote the experimental data, while solid line shows the
359 homogenous line. It is observed that experimental data is overestimated by Nicklin
360 (1962) correlation, due to improper drift velocity expression introduced in this
361 correlation which does not take into account the viscous and surface tension effects.
362 However, the proposed model ($U_t=1.2 \cdot J_t$) for bubble translational velocity gives a
363 satisfactory agreement, which is exactly equivalent to the model proposed by Wallis
364 (1969). The experimental data of bubble velocity as a function of $\varepsilon_{Lg}=J_g/J_L$ is presented
365 in Fig. 5 for different gas superficial velocities ranging from 0.38 m s^{-1} to 2.10 m s^{-1} . It
366 is interesting to see how data tends to be aligned in a regular trend, depending upon
367 superficial gas velocity. However, a slight scattering tendency is observed at higher J_g
368 which might be due to measurement uncertainty caused by the increasing flow
369 disturbances. In Fig. 5 the data trends validated the assumption of equivalent two-phase
370 flow where oil and water flow as a homogeneous mixture with the distribution
371 parameter equal to 1.2, in line with the works of Zuber and Findlay (1965) as well as
372 Wallis (1969). The agreement between proposed models and experimental data is
373 excellent: $e_{ri}=2.5 \%$, $\varepsilon=2.8 \%$.

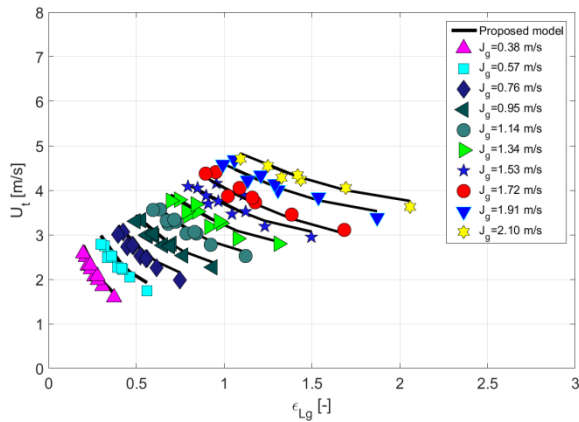
374



375

376

Fig. 4 Bubble translational velocity (U_t) versus mixture superficial velocity (J_t)



377

378

Fig 5. Translational bubble velocity (U_t) versus ϵ_{Lg} (ratio between superficial gas velocity and

379

superficial liquid velocity) for $J_g=0.38-2.10 \text{ m s}^{-1}$

380 2.7 Slug unit length

381

As there is no information regarding slug unit (cell) length, l_u for viscous oil-water-gas

382

flow in the open literature, a model for l_u is formulated so that the slug unit length acts

383

as an input parameter in the mechanistic model. The slug unit length is expressed

384

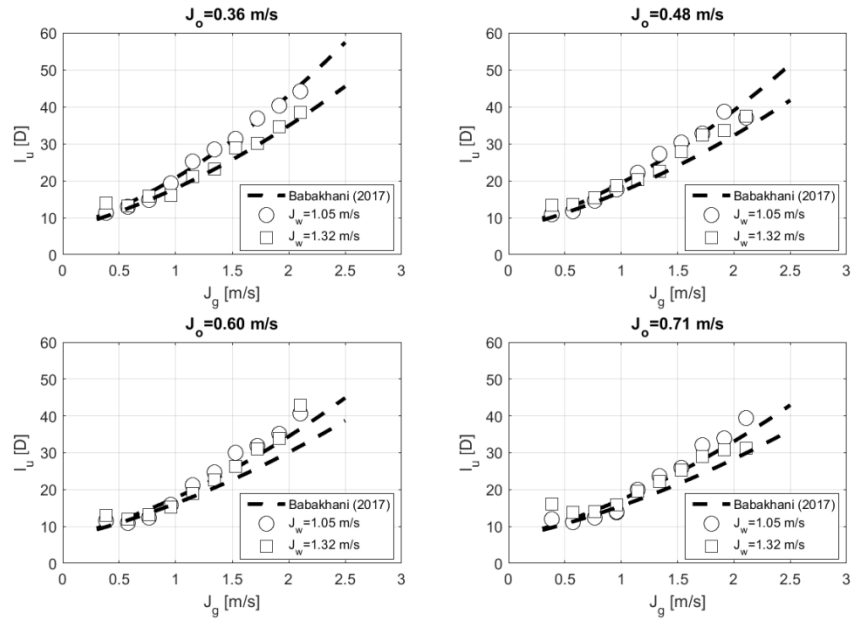
taking into account the influences of pipe diameter and operating conditions, based on

385

a power law functional form:

386
$$\frac{l_u}{D} = C \cdot (1 + \varepsilon_{LG})^n \quad (31)$$

387 From regression analysis, the coefficients C and n were found to be 7.3 and 2.0,
388 respectively. Babakhani (2017) and Babakhani et al. (2019) report a discussion about
389 statistical significance of the collected data. In particular, the slug body length l_s shows
390 a log-normal distribution, which shifts from right-skewed to normal like one as the gas
391 superficial velocity is increased at constant oil and water superficial velocities. The
392 mean slug body length increases from 3D to 27D, with a ratio between the standard
393 deviation and the mean varying within about 0.20 and 0.33. It is evident that for each
394 operating condition, l_s and l_u , as a consequence, are significantly variable. Nonetheless,
395 owing to their statistical distribution it make sense to adopt the mean value as
396 representative of the typical slug in a quasi-steady state model, at least in a range of
397 operating conditions where the translational bubble velocity is well correlated to ε_{LG} , as
398 shown in Fig. 5. This implies that an equivalent liquid phase with suitable averaged
399 properties is able to catch the more complex behavior of the two liquid phases (oil and
400 water) and that it is reasonable to adopt empirical models developed for two-phase slug
401 flows as closure relations. Fig. 6 shows comparison of measured slug cell length with
402 eq. 31, considering four different superficial oil velocities ($J_o=0.36-0.48-0.60-0.71 \text{ m}\cdot\text{s}^{-1}$),
403 parameterized by two water superficial velocities ($J_w=1.05-1.32 \text{ m}\cdot\text{s}^{-1}$). An
404 increasing dependence of slug cell length on superficial gas velocity is observed. An
405 analysis of 124 data points revealed that the agreement between experimental data and
406 proposed model by Babakhani (2017) was reasonable: Mean Average Percentage Error
407 (MAPE) resulted 10.3 %, and the standard deviation of the error was 9.5 %.



408

409

Fig. 6 Slug cell length versus superficial gas velocity for $J_o=0.36-0.71 \text{ m/s}^{-1}$

410

411

412 3. Solution procedure

413 In order to solve continuity and momentum equations of intermittent flow based on mechanistic

414 model (sections 2-1 to 2-3), some closure relationships are required. This information are

415 obtained from empirical correlations for two-phase flows because no references are available for

416 some parameters such as slug length, slug body holdup, and friction factor for liquid-liquid-gas

417 flows (a detailed description of models for two-phase flows are described in sections 2-4 to 2-7).

418 It is worth noting that the following assumptions are made to use mechanistic model:

419

- 420 • Uniform liquid height, that is, $\frac{\partial h_L}{\partial x} = 0$
- 421 • Oil and water are assumed to be a homogeneous mixture
- 422 • Gas is entrained and dispersed into slug body
- 423 • Entrained gas into slug body move with the velocity equals to Translational bubble
- 424 velocity
- 425 • Gas expansion will not occur from the pipe inlet
- 426 • Elongated bubbles move with a so-called translational bubble velocity ($U_g=U_t$)

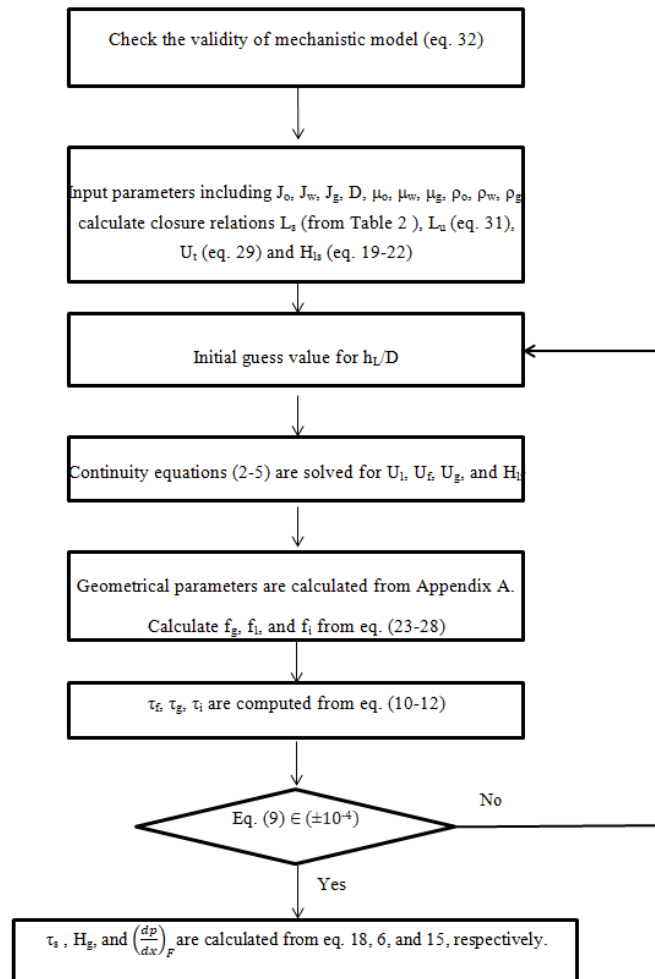
427 Based on the balance between the total free-surface energy of dispersed gas bubbles and the total
 428 kinetic turbulent energy of liquid in slug body, Zhang and Sarica (2006) proposed a criterion
 429 when the assumption of an equivalent liquid for oil and water is valid:

$$430 \quad J_L > \left(\frac{6.325 C_e \varphi_{Int} [\sigma_{ow} (\rho_w - \rho_o)]^{0.5}}{f_{LM} \rho_L} \right)^{0.5} \quad (32)$$

$$431 \quad C_e = \frac{2.5 - |\sin(\theta)|}{2}$$

432 Where θ , φ_{Int} , and σ_{ow} are pipe inclination, the volumetric fraction of dispersed phase, that is, oil
 433 in the present study ($\varphi_{Int} = \epsilon_{Lo} = J_o / (J_o + J_w)$), and interfacial tension between oil and water,
 434 respectively. The friction factor for liquid mixture (f_{LM}) is obtained from Blasius formulation
 435 (eq. 23 and 24), taking into account Reynolds number for homogeneous mixture of oil and water.
 436 This correlation is widely used to compute friction factor for oil-water flow (see, e.g. Colombo et
 437 al., 2017). A flowchart for calculation of pressure drop and gas holdup based on mechanistic
 438 model for three-phase intermittent flow, considering fully mixed oil/water and core-annular is
 439 shown in Fig. 7. The solutions of continuity and momentum equations only require rheological
 440 properties of phases, pipe diameter, and flow conditions.

441



442

443 **Fig. 7** Flowchart calculation of three-phase intermittent flow based on mechanistic model

444

445 **4. Validation of mechanistic model**

446 In the following sections, the results of three-phase pressure drop and gas holdup predicted by
447 mechanistic model are presented.

448

449

450

451

452 **4.1 Pressure drop prediction**

453 As no independent data set of pressure drop was available for viscous oil-water-gas to
454 validate the model, only two sets of experimental data are found to evaluate the model
455 performance. One data set is the experimental data of Babakhani (2017). Four values of
456 oil superficial velocity ($J_o=0.36, 0.48, 0.60, 0.71$ m/s) were considered, for each pair of
457 J_o - J_w the values of superficial gas velocity ranging from 0.22-1.91 were investigated.
458 Another source is data bank in the work of Poesio et al. (2009) who performed tests
459 with $\mu_o=1.2$ Pa.s within a 21 mm i.d. horizontal pipe. The details of data bank are
460 reported in Table 3.

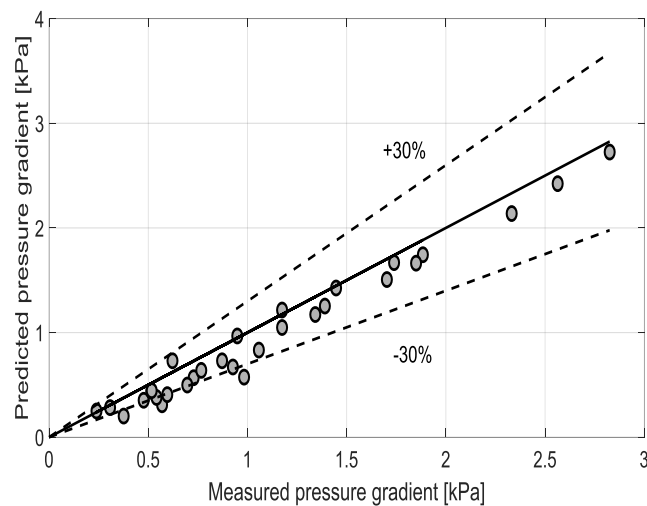
461 **Table 3.** Details of data sources used to evaluate model performance

Data source	Diameter [m]	Oil viscosity [Pa.s]	Gas velocity [m/s]	Liquid velocity [m/s]	Data points
Babakhani (2017)	0.040	0.83 @ room temp	0.22-1.91	1.02-2.05	131
Poesio et al. (2009)	0.021	1.2	0.29	0.13-3.4	30

462

463 As it is evident from Fig. 8, there is a fairly good agreement between predicted and
464 measured pressure drop data of Poesio et al. (2009), considering the average relative
465 error of -14.8% and standard deviation 14.7%. Almost all data predicted by the model
466 are underestimated measurements. Considering acceleration pressure drop contribution
467 in equation 14 might result in a better prediction of measured data by model and can be

468 a topic of further investigation. About 87% of all data predicted by the model falls
469 within $\pm 30\%$ of relative error. Larger deviation occurs at low oil superficial velocity.
470 At low oil superficial velocity, oil and water tends to form core-annular flow and
471 degree of stratification increases. Since the present model assumes an equivalent liquid
472 for oil and water, which oil and water treated as a fully-mixed liquid, it is possible that
473 the pressure drop predicted by the model shows slightly higher deviation.



474

475 **Fig 8.** Pressure drop comparison between prediction and data of Poesio et al (2009) for
476 $D=21\text{mm}$

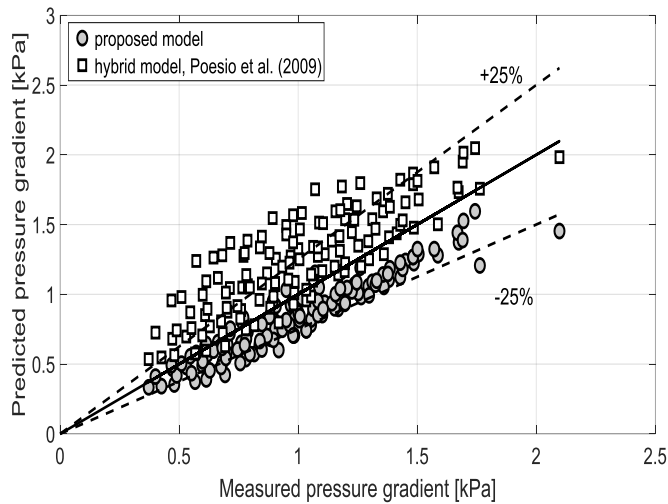
477 The comparison of pressure gradient computed by model and measured data by Babakhani
478 (2017) is depicted in Fig. 9 showing a good agreement with an average relative error of -15.4% ,
479 while standard deviation was found to be 10.2% . The wide range of operating conditions was
480 considered for this comparison. To evaluate the performance of current mechanistic model,
481 hybrid model developed by Poesio et al. (2009) is also compared in Fig. 9. They used Lockhart-
482 Martinelli parameter (χ) modified by Chisholm (1973) to predict three-phase pressure drop. The
483 hybrid model is based on solution of two-fluid model for liquid-liquid developed by Brauner

484 (1991), which is eventually substituted in Lockhart-Martinelli parameter to compute overall
 485 pressure drop. Table 4 lists the equations required for the hybrid model proposed by Poesio et al.
 486 (2009).

487 **Table 4.** Hybrid model proposed by Poesio et al. (2009)

Hybrid model	Additional information
$\Delta P_{o-w-g} = \phi_g^2 \cdot \Delta P_g$	$\chi = \sqrt{\frac{\Delta P_{tiq}}{\Delta P_g}}, C=15$
$\phi_g^2 = 1 + C \cdot \chi + \chi^2$	(Lockhart-Martinelli parameter)

488



489

490 **Fig 9.** Predicted pressure drop versus measured data of Babakhani (2017) and
 491 comparison with hybrid model developed by Poesio et al. (2009)

492 The proposed mechanistic model is able to predict pressure drop better than hybrid model over
 493 entire range of operating conditions. Almost 84% of all data fall within 25% of relative error for

494 proposed model while 54% of all data falls into 25% of relative error predicted by hybrid model.
495 Table 5 shows statistical analysis of proposed model and comparison with hybrid model.

496

497 **Table 5.** Comparison of pressure drop between proposed mechanistic model and hybrid
498 model

Models	e_{ri} (%)	Max e_{ri} (%)	Min e_{ri} (%)	Std deviation (%)
Poesio et al. (2009)	27.9	116	-13.1	26.4
Proposed model	-15.4	8.7	-39.1	10.2

499

500 The results of pressure drop prediction shows that in spite of complexity of three phase
501 flow of high viscous oil-water-gas, the developed mechanistic model is able to predict
502 pressure gradients with a reasonable average relative error. Hence, it can be used as an
503 operative engineering tool to compute pressure drop.

504 **4.2 Gas holdup prediction**

505 As no time-space average technique for measuring gas hold up has been so far
506 presented for viscous oil-water-gas flow in the open literature, all the comparisons of
507 model performance was made, taking into account the definition of translational bubble
508 velocity, that is, $H_g = J_g / U_g$ with $U_g = U_t$, reported in Table 6. Hence, the proposed model
509 is based on a drift-flux concept with distribution parameter equals to 1.2 (eq. 6), which
510 is derived from experimental analysis and it can be used as a reference value. A

511 comparison has been made between prediction of gas holdup by eq. (6) and available
 512 models in literature for two-phase flow of gas-liquid to check the possibility to use in
 513 three-phase flow. The 68 void fraction correlations according to large data set have
 514 been reported by Melkamu and Ghajar (2007). Among all correlations presented in
 515 their work, three correlations in the families of slip ratio models (Lockhart and
 516 Martinelli, 1946, and Chen, 1986) and $K_{\epsilon H}$ (Armand, 1946) are widely used. The latter
 517 was validated by Guilizzoni et al. (2018) who proposed an image-based technique by
 518 video camera, with a resolution of 1280×720 and frequency 50 fps, to measure average
 519 gas hold up. They concluded that Armand (1946) correlation has an outstanding
 520 performance, with mean average percentage error=3.1 % and $\epsilon=2.5$ %.

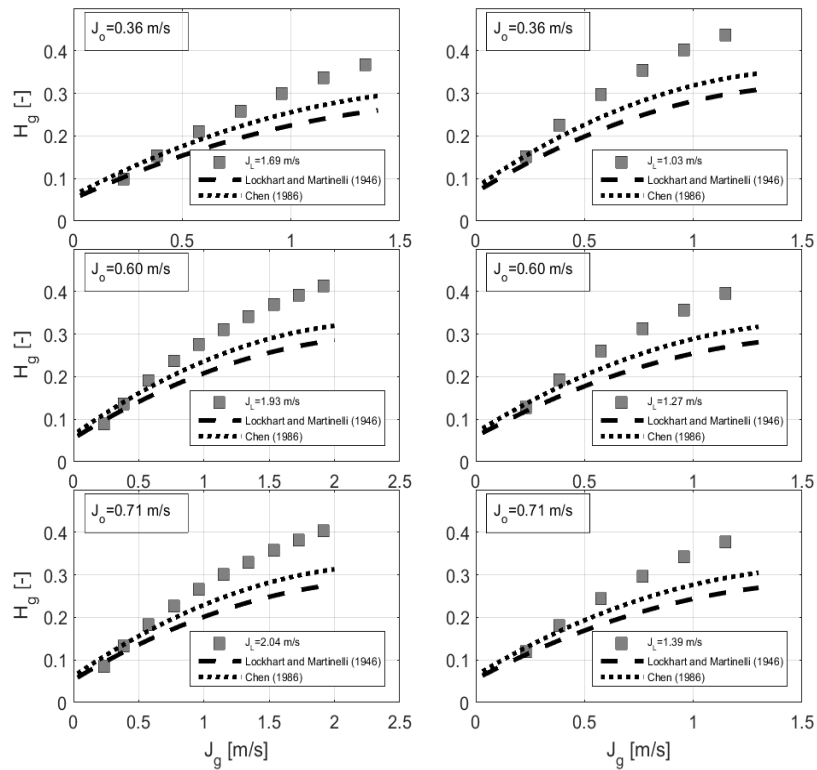
521 **Table 6.** Performance of available correlations for mean gas holdup

Correlation	Avg absolute error (%)	Max absolute error (%)	St deviation (%)
Lockhart and Martinelli (1946)	24.0	32.1	8.9
Chen (1986)	16.1	23.6	6.6

522

523 Comparison between average gas hold up (eq. 6) and correlations of Lockhart and
 524 Martinelli (1946) and Chen (1986) for $J_o=0.36-0.71$ m/s are shown in Fig. 10. Both
 525 models underestimated the reference value, with larger deviation at higher superficial
 526 gas velocity. Fig. 10 and Table 6 revealed that although these models are on basis of
 527 slip ratio concept, they are incapable of predicting mean average hold up.

528



530

531 **Fig 10.** Comparison between average gas hold up at $J_o=0.36-0.71$ m/s and correlations
 532 of Lockhart and Martinelli (1946), and Chen (1986)

533 **5.Conclusion**

534 A mechanistic model based on the solution of continuity and momentum equations is
 535 proposed to compute phase velocity and pressure drop in slug body and film section
 536 (assuming uniform liquid height) for horizontal viscous oil-water-air flows at
 537 atmospheric pressure. The model requires the superficial velocity of phases and
 538 rheological properties as input parameters. Oil and water are treated as an equivalent
 539 fluid with suitably averaged properties. In particular, density was determined by
 540 assuming homogeneous distribution, whereas viscosity was calculated according to

541 Einstein's equation. Accordingly, empirical closure relations for gas-liquid flows (slug
542 length and holdup) were used, due to the lack of information for viscous oil-water-gas
543 flows. The major output of mechanistic model is the pressure drop across slug unit cell.
544 Moreover, a correlation for calculation of mean gas holdup based on drift-flux concept
545 is also proposed. The results of the predicted pressure drop were compared with the
546 measurements reported in the literature survey, showing a promising approach for
547 viscous oil-water-gas phase flows in horizontal pipes, under a variety of operating
548 conditions where the statistical distribution of slug lengths indicates that the mean
549 value is representative of a typical slug structure in a quasi-steady state model.
550 Furthermore, it has to be taken into account that the current database available for
551 validation is relatively scarce and all the experiments on three-phase flows were
552 conducted in plants with a "smooth" introduction of the phases. Accordingly, it was not
553 possible to investigate the effect of the inlet conditions on the flow development. In
554 particular, the proposed approach seems to be valid until the translational bubble
555 velocity is well correlated to the liquid-to-gas input volume fraction, which implies that
556 the two liquids can be lumped into an equivalent liquid phase with suitable averaged
557 properties.

558 **Appendix A. Geometrical parameters**

559 The geometrical parameters, $A_f, A_g, S_f, S_g, S_i, H_{lf}$ are presented by Aziz and Govier
560 (1972), assuming that interface between gas-liquid is flat. They are all functions of
561 liquid film height (h_L) given by:

$$562 \quad \alpha = 2\cos^{-1}\left[1 - \frac{2h_L}{D}\right] \quad (\text{A-1})$$

563 $A_f = \frac{A}{2\pi}(\alpha - \sin \alpha)$ (A-2)

564 $A_g = A - A_f$ (A-3)

565 $H_{lf} = \frac{A_f}{A}$ (A-4)

566 $s_f = \frac{D\alpha}{2}$ (A-5)

567 $s_g = \pi D - s_f$ (A-6)

568 $s_i = 2D\sqrt{\left[\frac{h_L}{D} - \left(\frac{h_L}{D}\right)^2\right]}$ (A-7)

569

570

571 **Appendix B. Statistical parameters**

572 The statistical parameters based on average relative error and standard deviation is used

573 to evaluate performance of model with measured data as follows:

574 $e_{ri} = \frac{(E_{i,cal} - E_{i,meas})}{E_{i,measured}} \times 100$ (B-1)

575 $e = \frac{1}{N} \sum_{i=1}^N e_{ri}$ (B-2)

576 Standard deviation related to average relative error is:

577 $\varepsilon = \sqrt{\frac{\sum_{i=1}^N (e_{ri} - e)^2}{N-1}}$ (B-3)

578

579

580

581

582
583
584
585
586
587

588
589
590
591
592
593
594
595
596
597
598
599
600
601
602
603
604
605
606
607
608
609
610

References

- Acikgoz, M., Franca, F., Lahey JR, R.T. (1992). An experimental study of three-phase flow regimes. *International Journal of Multiphase Flow*, 18, 327-336.
- Al-Safran, E., Gokcal, B., Sarica. C. (2011). High viscosity liquid effect on two-phase slug length in horizontal pipes. *Presented at the 15th International Conference on Multiphase Production technology*. Cannes, France, Jun 15-17.
- Al-Safran, E., Kora, C., Sarica C. (2015). Prediction of slug liquid holdup in high viscosity liquid and gas two-phase flow in horizontal pipes. *Petroleum Science and Engineering*, 133, 566-575.
- Andreussi, P., Minervini, A., Paglianti, A. (1993). Mechanistic model of slug flow in near-horizontal pipes. *AICHE*, 39.
- Andritsos, N., Hanratty, T.J. (1987). Influence of interfacial waves in stratified gas-liquid flows. *AICHE*, 33, 444-454.
- Armand, A. (1946). The resistance during the movement of a two-phase system in horizontal pipes. *Izv Vse Tepl Inst*, 1, 16-23.
- Arney, M.S., Bai, R., Guevara, E., Joseph, D.D., Liu, K. (1993). Friction factor and holdup studies for lubricated pipelining- I experiments and correlations. *Internation Journal of Multiphase Flow*, 19, 1061-1076.
- Babakhani Dehkordi, P., Azdarpour, A., Mohammadian, E. (2018). The hydrodynamic behavior of high viscous oil-water flow through horizontal pipe undergoing sudden expansion- CFD study and experimental validation. *Chemical Engineering Research and Design I*, 39, 144-161.

611 Babakhani Dehkordi, P., Colombo, L.P.M., Guilizzoni, M., Sotgia, G. (2017a). CFD simulation
612 with experimental validation of oil-water core-annular flows through Venturi and Nozzle
613 flow meters. *Petroleum Science and Engineering*, 149, 540-552.

614 Babakhani Dehkordi, P., Colombo, L.P.M., Guilizzoni, M., Sotgia, G., Cozzi, F. (2017b).
615 Quantitative visualization of oil-water mixture behind sudden expansion by high speed
616 camera. *Physics: Conference Series*, 882.

617 Babakhani, P. (2017). *PhD thesis: Experimental and numerical analysis of multiphase flow*
618 *within horizontal pipeline with variable cross-sectional area*. Politecnico di Milano,
619 Milan, Italy.

620 Bannwart, A.C., Rodriguez, O.M.H., Trevisan, F.E. (2009). Experimental investigation on
621 liquid-liquid-gas flow: Flow patterns and pressure gradient. *Journal of Petroleum Science*
622 *and Engineering*, 65, 1-13.

623 Bannwart, A.C., Rodriguez, O.M.H., Trevisan, F.E., Vieira, F.F., De Carvalho, C.H.M. (2004).
624 Flow patterns and pressure gradients in horizontal upward inclined and vertical heavy oil-
625 water-gas flows: experimental investigation and full-scale experiments. *3rd International*
626 *Symposium on Two-Phase Flow Modelling and Experimentation*. Pisa, Italy.

627 Barnea, D., Brauner, N. (1985). Holdup of the liquid slug in two phase intermittent flow.
628 *International Journal of Multiphase Flow*, 11, 43-49.

629 Benjamin, T. (1968). Gravity currents and related phenomena. *Fluid Mech*, 31, 209-248.

630 Brauner, N. (1991). Two phase liquid-liquid annular flow. *Int.J.Multiphase Flow*, 17, 59-76.

631 Charles, M.E, Govier, G. t, Hodgson, G. (1961). The horizontal pipeline flow of equal density
632 oil-water mixtures. *The Canadian Journal of Chemical Engineering*, 39 (1), 27-36.

633 Chen, J.J.J. (1986). A further examination of void-fraction in annular two-phase flow.
634 *International Journal of Heat Mass Transfer*, 29, 1760-1763.

635 Chisholm, D. (1973). Pressure gradients due to friction during the flow of evaporating two-phase
636 mixtures in smooth tubes and channels. *Int. J. Heat Mass Transfer*, 16, 347-358.

637 Colombo, L.P.M., Guilizzoni, M., Sotgia, G., Babakhani Dehkordi, P., Lucchini, A. (2017).
638 Water holdup estimation from pressure drop measurements in oil-water two-phase flows
639 by means of the two-fluid model. *Physics: Conference Series*, 923.

640 Colombo, L.P.M., Guilizzoni, M., Sotgia, G.M., Marzorati, D. (2015). Influence of sudden
641 contractions on in situ volume fractions for oil-water flows in horizontal pipes. *Journal of*
642 *Heat and Fluid Flow*, 53, 91-97.

643 Einstein, A. (1906). Eine neue bestimmung der molekuldimensionen. *Ann. Phys*, 324, 289-306.

644 Grassi, B., Strazza, P., Poesio, P. (2008). Experimental validation of theoretical models in two-
645 phase high-viscosity ratio liquid-liquid flows in horizontal and slightly inclined pipes.
646 *International Journal of Multiphase Flow*, 34, 950-965.

647 Guilizzoni, M., Baccini, B., Sotgia, G., Colombo, L.P.M. (2018). Image-based analysis of
648 intermittent three-phase flow. *International Journal of Multiphase Flow*, 107, 256-262.

649 Hall, A. (1992). *Multiphase flow of oil, water and gas in horizontal pipes. Ph.D thesis*. Imperial
650 college. London, UK.

651 Hanich, L., Thompson, R. (2001). Validation of a novel algorithm for the adaptive calculation of
652 transient stratified flow of gas, oil and water in pipelines. *Int. J. Numeric. Meth. Eng*, 51,
653 579-607.

654 Hewitt, G. (2005). Three-phase gas-liquid-liquid flows in the steady and transient states. *Nuclear
655 Engineering and Design*, 235, 1303-1316.

656 Khor, S.H., Mendes-Tassis, M.A., Hewitt, G.F. (1997). One-dimensional modelling of phase
657 holdups in three-phase stratified flow. *Int. J. Multiphase Flow*, 23, 885-897.

658 Kowalski, J.E. (1987). Wall and interfacial shear stress in stratified flow in a horizontal pipe.
659 *AIChE*, 33, 274-281.

660 Laflin, G.C., Oglesby, K.D. (1976). *An experimental study on the effects of flow rate, water
661 fraction and gas/liquid ratio on air-oil-water flow in horizontal pipes. BS thesis*. U. of
662 Tulsa, Tulsa.

663 Lockhart, R.W., Martinelli, R.C. (1946). Proposed correlation of data for isothermal two-phase,
664 two component flow in pipe. *Chem. Eng. Progr*, 45, 39-48.

665 Loh, W.L., Premanadhan, V.K. (2016). Experimental investigation of viscous oil-water flows in
666 pipeline. *Journal of Petroleum Science and Engineering*, 147, 87-97.

667 Losi, G., Arnone, D., Corraera, S., Poesio, P. (2016b). Modelling and statistical analysis of high
668 viscosity oil/air slug flow characteristics in a small diameter horizontal pipe. *Chemical
669 Engineering Science*, 148, 190-202.

670 Losi, G., Poesio, P. (2016). An experimental investigation on the effect of viscosity on bubbles
671 moving in horizontal and slightly inclined pipes. *Experimental Thermal and Fluid
672 Science*, 75, 77-88.

673 Melkamu, A. Woldesemayat., Ghajar. A.J. (2007). Comparison of void fraction correlations for
674 different flow patterns in horizontal and upward inclined pipes. *Int. J. Multiphase Flow*,
675 33, 347-370.

676 Nadler, M., Mewes, D. (1995). Effect of the liquid viscosity on the phase distribution in
677 horizontal gas-liquid slug flow. *Int. J Multiphase Flow*, 21, 253-266.

678 Nicklin, D. (1962). Two-phase bubble flow. *Chemical Engineering Science*, 17, 693-702.

679 Odozi, U. (2000). *Three-phase gas/liquid/liquid slug flow. Ph.D thesis*. Imperial college.
680 London, UK.

681 Pan, L. (April 1996). *High pressure three-phase (gas/liquid/liquid) flow*. Ph.D. Thesis,
682 University of London.

683 Picchi, Davide., Strazza, D., Demori, M., Ferrari, V., Poesio, P. (2015). An experimental
684 investigation and two-fluid model validation for dilute viscous oil in water dispersed pipe
685 flow. *Experimental Thermal and Fluid Science*, 60, 28-34.

686 Poesio, P., Strazza, D., Sotgia, G. (2009). Very viscous oil/water/air flow through horizontal
687 pipes:Pressure drop measurement and prediction. *Chemical Engineering Science*, 64,
688 1136-1142.

689 Shi, J., Gourma, M., Yeung, H. (2017). CFD simulation of horizontal oil-water flow with
690 matched density and medium viscosity ratio in different flow regimes. *Journal of*
691 *Petroleum Science and Engineering*, 151, 373-383.

692 Shmueli, A., Unander, T.E., Nydal, O.J. (2015). Characteristics of gas/water/viscous oil in
693 stratified-annular horizontal pipe flows. *Offshore Technology Conference*. Rio de Janeiro,
694 Brazil.

695 Sotgia, G., Tartarini, P., Stalio, E. (2008). Experimental analysis of flow regimes and pressure
696 drop reduction in oil-water. *International Journal of Multiphase Flow*, 1161-1174.

697 Taitel, Y., Barnea, D. (1990). Two-phase slug flow. *Advances in heat transfer*, 20.

698 Taitel, Y., Barnea, D., Brill, J.P. (1995). Stratified three phase flow in pipes. *Int. J. Multiphase*
699 *Flow*, 21, 53-60.

700 Taitel, Y., Dukler, A.E. (1976). A model for predicting flow regime transitions in horizontal and
701 near horizontal gas-liquid flow. *AICHE*, 22, 47-55.

702 Wallis, G. (1969). *One dimensional Two-phase flow*. New York: McGraw-Hill.

703 Wang, S., Zhang, H.-Q., Sarica, C., Pereyra, E. (2013). Experimental study of high-viscosity
704 oil/water/gas three-phase flow in horizontal and upward vertical pipes. *SPE production*
705 *and operation*, 28(03), 306-316.

706 Zhang, H.Q., Wang, Q., Sarica, C., Brill, J.P. (2003a). Unified model for gas-liquid pipe flow via
707 slug dynamics- part 1: Model development. *Journal of Energy Resources and*
708 *Technology*, 125.

709 Zhang, H-Q., Sarica, C. (2006). Unified Modeling of Gas/Oil/Water Pipe Flow - Basic
710 Approaches and Preliminary Validation. *Society of petroleum engineers*, 1(02), 1-7.

711 Zhao, Y., Lao, L., Yeung, H. (2015). Investigation and prediction of slug flow characteristics in
712 highly viscous liquid and gas flows in horizontal pipes. *Chemical Engineering Research*
713 *and Design*, 102, 124-137.

714 Zhao, Y., Yeung, H., Lao, L. (2013b, May). High liquid viscosity effects on wall and interfacial
715 shear stresses in horizontal liquid-gas flows. *Proceedings of the 8th International*
716 *Conference on Multiphase Flow, ICMF*, 26-31.

717 Zuber, N., Findlay, J.A. (1965). Average volumetric concentration in two-phase flow systems. *J.*
718 *Heat Transfer*, 87, 453-468.

719

720

721

722

723

724

725